Multiplex genome editing of mammalian cells for producing recombinant heparin

Bryan E. Thacker [a], Kristen J. Thorne [a], Colin Cartwright [a], Jeeyoung Park [a], Kimberly Glass [a], Annie Chea [a], Benjamin P. Kellman [b], Nathan E. Lewis [b], Zhenping Wang [c], Anna Di Nardo [c], Susan T. Sharfstein [d], Walter Jeske [e], Jeanine Walenga [e], John Hogwood [f], Elaine Gray [f], Barbara Mulloy [f], Jeffrey D. Esko [g,h], Charles A. Glass [a,*]

[a] TEGA Therapeutics Inc, 3550 General Atomics Court, G02-102, San Diego, CA, 92121, USA
[b] Departments of Pediatrics and Bioengineering, University of California, San Diego, 9500 Gilman Drive, La Jolla, CA, 92093, USA
[c] Department of Dermatology, University of California, San Diego, School of Medicine, 9500 Gilman Drive, La Jolla, CA, 92093, USA
[d] College of Nanoscale Science and Engineering, SUNY Polytechnic Institute, 257 Fuller Road, Albany, NY, 12203, USA
[e] Cardiovascular Research Institute, Loyola University Chicago, Health Sciences Division, 2160 S 1st Avenue, Maywood, IL, 60153, USA
[f] National Institute for Biological Standards and Control, Blanche Lane, South Mimms, Herts, EN6 3QG, UK
[g] Glycobiology Research and Training Center, University of California, San Diego, 9500 Gilman Drive, La Jolla, CA, 92093, USA
[h] Department of Cellular and Molecular Medicine, University of California, San Diego, 9500 Gilman Drive, La Jolla, CA, 92093, USA

ARTICLE INFO

ABSTRACT

Heparin is an essential anticoagulant used for treating and preventing thrombosis. However, the complexity of heparin has hindered the development of a recombinant source, making its supply dependent on a vulnerable animal population. In nature, heparin is produced exclusively in mast cells, which are not suitable for commercial production, but mastocytoma cells are readily grown in culture and make heparan sulfate, a closely related glycosaminoglycan that lacks anticoagulant activity. Using gene expression profiling of mast cells as a guide, a multiplex genome engineering strategy was devised to produce heparan sulfate with high anticoagulant potency and to eliminate contaminating chondroitin sulfate from mastocytoma cells. The heparan sulfate purified from engineered cells grown in chemically defined medium has anticoagulant potency that exceeds porcine-derived heparin and confers anticoagulant activity to the blood of healthy mice. This work demonstrates the feasibility of producing recombinant heparin from mammalian cell culture as an alternative to animal sources.

1. Introduction

The anticoagulant potency of heparin was discovered more than 100 years ago. It has since been used for decades as a life-saving drug to control blood coagulation during renal dialysis and cardiac surgery and in treatment of deep vein thrombosis and disseminated intravascular coagulopathies. Its importance is clearly evident by its inclusion on the World Health Organization's list of "essential medicines" (WHO, 2019) and by its widespread use, as hundreds of thousands of doses are administered daily world-wide. Heparin is a natural product derived primarily from porcine intestine with over 50% of the world's supply sourced as a byproduct of pork production in China where hundreds of millions of pigs are slaughtered annually.

Sourcing heparin from a single species puts the world supply at risk due to disease epidemics in the pig population. In 2007, massive outbreaks of porcine reproductive and respiratory syndrome resulted in a worldwide heparin shortage (McMahon et al., 2010; Mans et al., 2015; Kishimoto et al., 2008; Keire et al., 2015). Adulteration of heparin with non-naturally occurring over-sulfated chondroitin sulfate (OSCS) led to over 200 deaths worldwide and more than 800 reports of serious hypertension and adverse allergic reactions in 2008. The Food and Drug Administration in the United States continues to address concerns about foreign heparin production and its quality control (Committee on Energy and Commerce, 2016). The vulnerability of the heparin supply chain continues to be a concern, especially in the wake of the current African Swine Fever epidemic that has claimed over 32% of China's pig herd since August 2018 (Market Report, 2020). The frequency of porcine epidemics suggests that the supply of animal sourced heparin will continue to be at risk.

Abbreviations

APTT	activated partial thromboplastin time
BMDC	bone marrow derived cells
CS	chondroitin sulfate
FPKM	fragments per kilobase of transcript per million mapped reads
GlcA	glucuronic acid
GlcNAc	*N*-acetylglucosamine
GlcNS	*N*-sulfoglucosamine
HS	heparan sulfate
IdoA	iduronic acid
IIa	Factor IIa
LC/MS	liquid chromatography/mass spectroscopy
MST	mastocytoma
OSCS	over-sulfated chondroitin sulfate
UFH	unfractionated heparin
USP	United States Pharmacopeia
Xa	Factor Xa

Modern synthetic biology capabilities suggest that engineered mammalian cells could provide an alternative source of heparin. Unlike proteins expressed by a single gene, heparin, a polysaccharide, is produced in a metabolic pathway involving over 20 enzymes (Kreuger and Kjellen, 2012), possibly requiring a multiplex genome engineering approach (Glass, 2018). Heparin is a form of heparan sulfate (HS), which is produced by all types of animal cells, but differs in the degree of sulfation and the level of anticoagulant activity (Xu and Esko, 2014). Heparin is made exclusively in granulated connective tissue type mast cells. Unfortunately, mast cells are difficult to propagate in cell culture and therefore, are not appropriate for commercial production. In contrast, HS can be produced in many types of cells used for recombinant protein production. Genetic engineering of the cells in turn allows manipulation of the HS structure, with the prospect of engineering cells to produce material with the structure and function of pharmaceutical heparin (Oduah et al., 2016).

Heparin and HS are structurally similar, consisting of a polysaccharide chain backbone composed of repeating alternating residues of α1,4-linked *N*-acetyl-D-glucosamine (GlcNAc) bound to β1,4-linked D-glucuronic acid (GlcA) residues. As the chains assemble, they undergo modifications that include *N*-deacetylation and *N*-sulfation of subsets of *N*-acetylglucosamine residues (catalyzed by 4 members of the *N*-deacetylase/*N*-sulfotransferase (NDST) family), C5 epimerization of the GlcA residues to L-iduronic acid (IdoA, catalyzed by glucuronyl C5-epimerase (GLCE)), *O*-sulfation of uronic acids (catalyzed by HS 2-*O*-sulfotransferase (HS2ST)) and of glucosamine residues (catalyzed by HS 6-*O*-sulfotransferase (HS6ST), 3 isozymes, and HS 3-*O*-sulfotransferase (HS3ST), 7 isozymes) (Kreuger and Kjellen, 2012; Thacker and Sharfstein, 2018) (Fig. 1a). Modification of the polysaccharide chains is not template driven and does not go to completion. Heparin and HS are therefore heterogeneous mixtures of polydisperse and variably modified chains. Top-down analysis of the sequence and domain structure of the chains is quite complex. Instead, bottom-up analyses of the chains are possible by degradation of the chains into disaccharides with bacterial heparin lyases or nitrous acid followed by chromatographic or electrophoretic separation of the differentially sulfated disaccharides (Deakin and Lyon, 2008; Lawrence et al., 2008a). The rules that determine the individual sulfation reactions are partially understood (e.g., *N*-sulfation precedes *O*-sulfation, IdoA is 2-*O*-sulfated much more frequently than GlcA and sulfation levels appear to be determined by the expression levels of the corresponding sulfotransferases) (Kreuger and Kjellen, 2012; Thacker et al., 2014). What determines the positioning and extent of sulfation and epimerization is not well understood (Kreuger and Kjellen, 2012).

Heparin is a highly sulfated form of HS, in which the vast majority of the disaccharides contain IdoA and *N*- and *O*-sulfate groups. Anticoagulant activity depends of the presence of a 3-*O*-sulfated *N*-sulfoglucosamine residue positioned within a preferred pentasaccharide sequence (GlcNAc6S-GlcA-GlcNS3S±6S-IdoA2S-GlcNS6S) (Fig. 1a) (Atha et al., 1985). The presence of this pentasaccharide in heparin or in HS confers the capacity to bind to antithrombin, which results in a striking enhancement in the ability of antithrombin to inactivate factor IIa (thrombin), factor Xa and other proteases in the coagulation cascade. Thus, one cell engineering strategy is to increase the antithrombin binding pentasaccharide by increasing the expression levels of the relevant sulfotransferases (Glass, 2018).
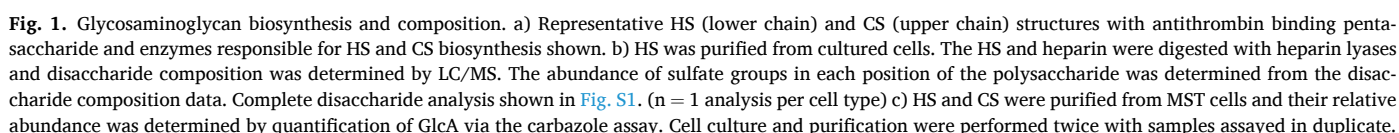
Repeated attempts to increase the anticoagulant activity to relevant levels in common bioproduction cell lines (i.e. CHO, HEK293) have been unsuccessful. Our experiments transfecting CHO and HEK293 cells with Hs3st1, Hs6st2, Ndst2 and serglycin never achieved anti-Xa activity above 20 U/mg, whereas the anti-Xa activity of pharmaceutical heparin is >180 U/mg. In published reports, overexpression of two critical enzymes for heparin production, NDST2 and HS3ST1, in CHO resulted in HS with high *N*-sulfate content (80–100 percent of disaccharides) but little *O*-sulfate (<10 percent of disaccharides). The HS bound antithrombin but had less than 5 percent of the anti-Xa specific activity of heparin (Baik et al., 2012). In other work, HEK293 cells were transfected to express the heparin core protein serglycin yielding HS with anticoagulant activity one-seventh that of pharmaceutical heparin (Lord et al., 2016). A naturally occurring mastocytoma (MST) cell line that is readily cultured in vitro produces HS with high sulfate content but no 3-*O*-sulfate and low anti-Xa activity (Montgomery et al., 1992). MST cells were transduced to express Hs3st1, which yielded 3-*O*-sulfated HS with significant anti-Xa activity that was still less than 25 percent of the specific activity of pharmaceutical heparin (Gasimli et al., 2014). These results suggest that increasing the expression of multiple HS biosynthetic genes (i.e. Hs3st1, Hs6sts and/or Ndsts) in MST cells could yield a potent anticoagulant. Despite the unknown regulatory and bioprocess challenges of a new cell line, MST cells were chosen for cell engineering.

Here we deployed a multiplex genome engineering strategy to create MST cell lines that produce highly sulfated HS with anticoagulant activities exceeding pharmaceutical heparin. Using gene expression profiling to guide the strategy, the biosynthetic pathways were engineered to eliminate production of contaminating chondroitin sulfate (CS) and to produce highly anticoagulant HS with a composition approximating porcine derived heparin. The cell line was also successfully adapted to serum-free medium in anticipation of commercial production.

2. Materials and methods

2.1. Cell culture

Cell lines derived from the Furth murine MST were previously described (Montgomery et al., 1992; Gasimli et al., 2014) and were grown in DME/F12 medium (1:1) (Cytiva) supplemented with 15% fetal bovine serum (FBS, BioWest). CHO–S cells (ThermoFisher) were grown in CD CHO medium (Gibco) with 8 mM GlutaMAX (Gibco). 293F cells (ThermoFisher) were grown in FreeStyle 293 medium (Gibco). HeLa–S3 cells (Sigma) were grown in EX-CELL HeLa medium (Sigma) with 6 mM GlutaMAX. Engineered MST cells were later grown in CD CHO, CDM4NS0 (Cytiva) and SFM4MAb (Cytiva) serum-free media. Cells were typically grown in 30 mL of culture medium in shaker flasks (125 rpm) at 37 °C, under 5% CO_2 in 95% air. Viable cell density was determined on each day using a hemocytometer and trypan blue. To assess cell line stability, the cell line was grown continuously in CDM4NS0 plus 6 mM GlutaMAX for 63 generations. Cells were frozen at 15, 32, 47 and 63 generations and then thawed to produce and characterize HS.

Fig. 1. Glycosaminoglycan biosynthesis and composition. a) Representative HS (lower chain) and CS (upper chain) structures with antithrombin binding penta-saccharide and enzymes responsible for HS and CS biosynthesis shown. b) HS was purified from cultured cells. The HS and heparin were digested with heparin lyases and disaccharide composition was determined by LC/MS. The abundance of sulfate groups in each position of the polysaccharide was determined from the disac-charide composition data. Complete disaccharide analysis shown in Fig. S1. (n = 1 analysis per cell type) c) HS and CS were purified from MST cells and their relative abundance was determined by quantification of GlcA via the carbazole assay. Cell culture and purification were performed twice with samples assayed in duplicate.

2.2. Gene expression profiling

Primary murine mast cells were generated by extracting bone marrow cells from the femurs of 5–8-week-old female mice and culturing the cells in RPMI 1640 medium (Gibco) supplemented with 10% inactivated FBS (ThermoFisher), 25 mM HEPES (pH 7.4), 4 mM L-glutamine, 0.1 mM nonessential amino acids, 1 mM sodium pyruvate, 50 μM β-mercaptoethanol, 100 IU/mL penicillin and 100 μg/ml strep-tomycin. Recombinant murine IL-3 (1 ng/mL; R&D Systems) and re-combinant murine stem cell factor (SCF; 20 ng/mL; R&D Systems), both shown to support the in vitro growth and differentiation of the mast cell precursor, were also included (Wang et al., 2012). Murine mast cells derived from bone marrow cells with SCF and IL-3 become mature after 4 weeks of culture in vitro. After 4 weeks, mast cells were consistently generated as confirmed by the expression of CD117 (c-Kit) and FcεRI by flow cytometry; cell maturation was confirmed by metachromatic staining with toluidine blue. The purity of mast cells was greater than 98%.

The disaccharide composition of HS purified from bone marrow derived cells (BMDC) at 0 to 4 weeks into the differentiation protocol was determined by liquid chromatography/mass spectrometry (LC/MS)

as previously described (Lawrence et al., 2008a). RNA was prepared from 0.5×10^6 undifferentiated and week 3 differentiated cells using the RNeasy kit (Qiagen) with RNase-Free DNase (Qiagen). MST cells grown in DME/F12 with 15% FBS were prepared in parallel for comparison. RNA sample quality was assessed by TapeStation (Agilent) with RNA Integrity Number greater than 8.0 deemed acceptable for generating sequencing libraries. The TruSeq Stranded mRNA Sample Prep Kit (Illumina) was used to generate sequencing libraries. RNA libraries were multiplexed and sequenced with 100 base pair paired end reads to a depth of approximately 50 million reads per sample on an Illumina HiSeq4000. Reads were aligned to the mouse (GRCm38.p6; GCF_000001635.26 (Church et al., 2011)) NCBI reference genome using default parameters for STAR v2.6.0c (Dobin et al., 2013). Alignment was performed after trimming for quality and adaptors using default pa-rameters with Trimmomatic v0.32 (Bolger et al., 2014). Counts were normalized for coverage and gene length to Fragments Per Kilobase of transcript per Million mapped reads (FPKM).

2.3. Heparan sulfate production

Cells were grown in suspension in shaker flasks. Cultures were

seeded at 0.2×10^6 cells/mL in 30 mL of culture medium in shaker flasks (125 mL) at 37 °C under an atmosphere of 5% CO_2/95% air for seven days. For larger preparations, cells were seeded in 100–300 mL of medium in multiple 1-liter flasks. Cells and medium were separated by centrifugation (9000 rpm, 10 min). The cell pellet was resuspended in 25 mM sodium acetate, pH 6.0, 0.25 M NaCl, 0.1% Triton X100 (wt/vol) and 0.5 mg/mL Pronase (Sigma) and incubated with shaking overnight at 37 °C. Conditioned medium and protease digested cells were filtered through a 0.45 μm PES filter and applied to 0.5 mL DEAE-Sephacel columns, equilibrated and washed with DEAE wash buffer (25 mM sodium acetate, pH 6.0, 0.25 M NaCl) and eluted with the same buffer containing 2 M NaCl. The eluate was desalted on PD10 columns (Cytiva) for small volumes or by dialysis for large volumes and then dried by lyophilization. The dried product was reconstituted in water, then digested with micrococcal nuclease (Worthington) overnight at 37 °C followed by Pronase digestion for 3 h at 37 °C. Beta-elimination was performed to liberate the HS from core protein by addition of NaOH to 0.4 M with overnight incubation at 4 °C. After the sample was neutralized with acetic acid, it was diluted with water and reapplied to DEAE-Sephacel, then washed and eluted as described above. The eluate was desalted and lyophilized. Protein and DNA content were measured with the BCA protein assay and by UV absorbance. The nuclease and Pronase digests were repeated as needed to eliminate residual nucleic acid or protein contamination.

2.4. Heparan sulfate characterization

HS was quantified using the carbazole assay (Bitter and Muir, 1962) with GlcA (Sigma) used to construct a standard curve. The mass of HS was calculated based on the GlcA quantity and the average disaccharide molecular weight of the preparation as determined by disaccharide composition analysis.

HS disaccharide composition was determined by digestion of the polysaccharide and quantification of the resulting disaccharides by UPLC (Deakin and Lyon, 2008). Briefly, 1 μg of HS was diluted to 120 μL in 40 mM ammonium acetate, 3.3 mM calcium acetate, pH 7.0 and treated with 2 mU each of heparin lyases I, II and III, overnight at 37 °C. The samples were then dried in a SpeedVac and reconstituted in 10 μL of 23.5 mM 2-aminoacridone in 85% DMSO/15% acetic acid and incubated at 37 °C for 10 min..NaBH$_3$CN (10 μL of 1 M in 85% DMSO/15% acetic acid) was added and the sample was incubated at 37 °C overnight. The reaction was terminated by addition of 180 μL of 50 mM acetic acid. Samples were loaded onto an Acquity UPLC (Waters) equipped with a fluorescence detector and a HSS C18 column (1.8 μm beads, 2.1 x 100-mm inner diameter) equilibrated in 0.1 M ammonium acetate. Disaccharides were resolved with a methanol gradient and were quantified relative to disaccharide standards (Iduron). In some cases, composition was determined by tagging the disaccharides with aniline instead of 2-aminoacridone and the disaccharides were quantified by LC/MS using isotopically labeled disaccharide standards for quantification (Lawrence et al., 2008a). In either UPLC or LC/MS analysis, the pmol of each type of disaccharide in the sample were determined by comparison to standards of known mass. The eight commonly occurring HS disaccharides can be detected using these methods. The relative abundance of each was calculated by dividing the pmol of each disaccharide by the total pmol of all disaccharides in the sample. Sulfate content per 100 disaccharides was determined by summing the percent abundance of each disaccharide carrying *N*-sulfate, 2-*O*-sulfate or 6-*O*-sulfate. Note that some disaccharides carry more than one sulfate group while others are devoid of sulfate. Sulfate content is depicted in the figures as the percentage of disaccharides in the sample carrying each type of sulfate group. 3-*O*-sulfate inhibits the heparin lyases used for this analysis leaving resistant tetrasaccharide digestion products, which are chemically unstable and for which the tetrasaccharide standards are not readily available (Huang et al., 2015). For detection of CS by LC/MS, glycosaminoglycans were purified from cell culture as described above for HS

and purified samples were digested with chondroitinase ABC (Amsbio), labeled with aniline and analyzed by LC/MS using CS standards. Relative abundance of HS versus CS was calculated from the GlcA contributed from purified HS and purified CS as measured by the carbazole assay.

To simplify their representation, disaccharides are labeled in the figures using a disaccharide structural code (Lawrence et al., 2008b). In this code, the $\Delta^{4,5}$-unsaturated uronic acid resulting from heparin lyase digestion is designated as D. For HS, the *N*-substituent on glucosamine is either A or S for acetate or sulfate, respectively. For CS, galactosamine is represented by a. The presence and location of ester-linked sulfate groups are depicted by the number of the carbon atom on which the sulfate group is located or by 0 if absent. For example, D2S6 refers to a disaccharide composed of 2-sulfo-$\Delta^{4,5}$-unsaturated uronic acid--*N*-sulfoglucosamine-6-sulfate. The presence of 3-*O*- and 6-*O*-sulfate on the same hexosamine is indicated by the number 9.

The anticoagulant activity of HS was determined using an anti-Xa assay. Human antithrombin (Enzyme Research Laboratories) was diluted to 66 μg/mL, Human factor Xa (Enzyme Research Laboratories) was diluted to 0.4 μg/mL and substrate S-2765 (Chromogenix) was diluted to 0.5 mg/mL in assay buffer (25 mM HEPES, pH 7.4, 150 mM NaCl, 0.1% BSA). For each sample, 5 ng of HS was diluted to 96 μL in assay buffer, then 24 μL of antithrombin was added and 50 μL of this solution was pipetted into duplicate wells of a 96-well plate. Factor Xa solution was added (50 μL) to each well followed by 50 μL of the substrate S-2765 10 min later. The hydrolysis of the substrate was measured at OD$_{450}$ and the rate of reaction was determined from the slope. A standard curve of pharmaceutical unfractionated heparin (APP Pharmaceuticals) was used to determine the anti-Xa activity of the samples. Anti-Xa yield was determined by multiplying the specific anti-Xa activity and the HS yield of the culture.

2.5. Genome engineering

Gene knockout was accomplished using CRISPR/Cas9 with sgRNAs designed using the CRISPR Design Tool and sgRNAs and Cas9 from Synthego. sgRNA sequences and the accession numbers of the genes used to design the sequences are shown in Table S1. sgRNAs were designed in pairs to excise large segments (>200 bp) of the gene to accelerate the identification of useful clones by PCR. To overexpress transgenes, transductions were performed using lentivirus produced by the UC San Diego Vector Development Core Laboratory with open reading frame and lentiviral constructs produced by GenScript. Accession numbers for the genes overexpressed are shown in Table S2.

Transductions and transfections were performed on MST cells grown in DME/F12 containing 15% FBS. Transductions were performed by spinoculation with 10^5 cells in 0.5 mL of growth medium plus 8 μg/mL polybrene and viral particles at MOI 100. Tubes were spun at $800 \times g$ for 20 min at room temperature, then the cells were transferred into fresh medium and cultured overnight. The cells were transferred to fresh medium again after 24 h. For CRISPR mediated knockout, transfections were performed on a Neon electroporation device (ThermoFisher) with 10^6 cells and 180 pmol each of paired sgRNAs and 20 pmol of Cas9 protein.

Successful gene mutations by CRISPR were verified by PCR on genomic DNA using primers that flank the mutation site (Table S3). Successful excision of a block of DNA resulted in a shift of the PCR product to a lower size on the gel. To determine the DNA sequence of the mutated region, PCR amplicons were purified using the QIAquick PCR Purification Kit (Qiagen), quantified using the AccuBlue High Sensitivity dsDNA Quantitation Kit (Biotium) and were submitted for Amplicon-EZ next generation sequencing (Azenta).

Verification of transgene integration was performed by PCR on genomic DNA. Rapid screening of colonies was performed using PCR primers complementary to the lentiviral construct sequences that flank the multiple cloning site ("pHIV7 lentiviral construct" primer set shown

in Table S2). This primer set could detect any transgene introduced via the lentiviral construct. Genotyping was performed in this way for both mixed populations and single cell-derived colonies. Gene specific verification was performed on genomic DNA with a forward primer complementary to the protein coding sequence and reverse primer complementary to the lentiviral backbone. (Table S2).

To verify transcription of the lentiviral transgenes, total RNA was extracted using the PureLink RNA Mini Kit (Invitrogen) and treated with DNase I, amplification grade (Invitrogen) according to the manufacturer's instructions. Then, cDNA was produced from the RNA using Thermo Maxima First Strand cDNA Synthesis Kit for RT-PCR (Thermo Fisher). Controls for contamination with genomic DNA were produced in parallel reactions without the reverse transcriptase. PCR was performed on the cDNA and controls using the primer sets shown in Table S2.

In some cases, protein expression of transgenes was verified by Western blotting. Total cell lysate was produced from cells grown in DME/F12 plus 15% FBS using RIPA buffer plus protease and phosphatase inhibitors. Protein content in the lysates was normalized after measurement with the BCA Protein Assay (ThermoFisher). 20 μg total protein from each lysate was prepared by boiling in NuPAGE LDS Sample Buffer plus beta-mercaptoethanol. Samples were run on a NuPAGE 4–12% Bis-Tris protein gel (Invitrogen) and transferred to Immobilon-FL PVDF membrane (MilliporeSigma). Membranes were blocked in Odyssey TBS Blocking Buffer (Li-Cor) and then incubated in primary antibodies for GAPDH (mAb, ab8245, Abcam), Hs6st1 (pAb, AF5057, R&D Systems) or Hs6st2 (pAb, AF2710, R&D Systems) and then IRDye-secondary antibodies (Li-Cor). The blots were imaged on a Li-Cor imaging system. Attempts to blot for Hs3st1 or Ndst2 using commercially available antibodies were not successful.

2.6. Screening colonies by heparan sulfate characterization

An abbreviated HS purification strategy was used to streamline colony screening for anti-Xa activity. Single cell colonies were grown in 6-well dishes containing 2 mL of DME/F12 plus 15% FBS for five days. In some cases, cell suspension (100 μL) was collected, washed in PBS, lysed and used for a BCA protein assay. The remaining content of the well was adjusted to 0.1% Triton X100 and 0.5 mg/mL Pronase and digested overnight at 37 °C. The digested product was passed over a bed of 100 μL DEAE-Sephacel, washed with DEAE wash buffer and eluted with 0.5 mL DEAE elution buffer. The eluate was used directly in the anti-Xa activity assay with an equal volume of DEAE elution buffer added to the standards. Activity was expressed as activity per well or normalized by cellular protein. After colonies of interest were identified using this method, the colonies were grown up in shaker flasks and the HS was prepared and characterized as described above.

2.7. Biological assays

2.7.1. In vitro

In vitro characterization of recombinant HS was performed at two independent facilities as shown in Table 1.

2.7.2. For the analysis with the international standard

Potencies of samples of unfractionated heparin (UFH) and B 7A HS were assessed against the 6th International Standard for UFH, 07/328. Antithrombin dependent anti-IIa, antithrombin dependent anti-Xa, heparin cofactor II dependent anti-IIa and activated partial thromboplastin time (APTT) were measured as previously described (Hogwood et al., 2018). Data analyses were carried out using the parallel line model in CombiStats 6.0. The weight average molecular weight was determined on the same samples using an Agilent GPC-50. The method as previously described (Mulloy et al., 2014) was used with the system calibrated by the current United States Pharmacopeia (USP) reference standard for UFH molecular weight calibration. The % of high

antithrombin-affinity material and the kallikrein generating capacity of the sample were accessed as described previously (Hogwood et al., 2018).

2.7.3. For the analysis with the USP standard

The anti-Xa and anti-IIa potencies of UFH (Medefil porcine mucosal heparin, lot# 13353) and B 7A HS were determined using commercially available chromogenic assays (Aniara, West Chester, OH). For these analyses, test agents were supplemented into citrated normal human pooled plasma. The potencies of each batch of test agent were calculated relative to the latest USP heparin standard using the slope-ratio method. The molecular weight profile of each B 7A HS was determined using the method reported previously (Ahsan et al., 1995). Analysis was carried out by injecting 20 μL of sample (10 mg/mL in 0.3 M sodium sulfate) into the HPLC system. The flow rate for the mobile phase (0.3 M sodium sulfate) was 0.5 mL/min and the run time for each sample was 65 min. UV detection was made at 205 nm. The elution profile of each sample was analyzed relative to a previously determined calibration curve made using 13 narrow range heparin fractions ranging in molecular weight from 51.0 kDa to 2.4 kDa. The weight average molecular weight (Mw) and polydispersity (Mw/Mn) was determined.

2.7.4. In vivo

The anticoagulant effect of HS was assessed in vivo by injection of C57BL/6J male mice (8 weeks of age) with PBS, 3 mg/kg UFH (APP Pharmaceuticals) or 3 mg/kg of B 7A HS (n = 4 per group) via subcutaneous injection. Blood was collected from tail incisions into tubes with sodium citrate at 30, 60 and 180 min after injection. The cells were removed by centrifugation and the supernatant blood plasma was assayed for anti-Xa activity as described in section 2.4.

2.8. Statistics

Error bars show standard error on all figures. For anti-Xa activity after in vivo administration statistical significance was determined by 2-way ANOVA with Bonferroni posttests with P < 0.05 considered statistically significant.

3. Results

3.1. Cell lines

All mammalian cells produce HS although the degree of sulfation and relative content of uronic acid epimers differs by cell type. The degree of sulfate content of HS is typically much less than that found in heparin. For example, each ng of HS from CHO cells contained 1.53 pmol of disaccharide with no sulfate, 0.71 pmol of disaccharide with *N*-sulfate, 0.32 pmol of disaccharide with 2-*O*-sulfate and 0.11 pmol of disaccharide with 6-*O*-sulfate. In contrast, for heparin each ng of heparin contained 0.13 pmol of disaccharide with no sulfate, 1.56 pmol of disaccharide with *N*-sulfate, 1.39 pmol of disaccharide with 2-*O*-sulfate and 1.56 pmol of disaccharide with 6-*O*-sulfate. Relative abundance of sulfate groups in each type of HS is shown in Fig. 1b. HeLa–S3 and 293F similarly have HS that is much less modified than porcine UFH. In contrast, HS produced by a mouse mastocytoma (MST) cell line has sulfate content comparable to heparin (Fig. 1b and S1) but lacks 3-*O*-sulfation and anticoagulant activity (Montgomery et al., 1992; Gasimli et al., 2014). MST cells grow in suspension and have been previously engineered by introduction of HS3ST1 in a partially successful attempt to make recombinant heparin (Montgomery et al., 1992; Gasimli et al., 2014).

3.2. Inactivation of chondroitin sulfate biosynthesis

Mammalian cells also produce CS, which co-purifies with HS and must be removed by exhaustive enzymatic digestion. Its production may

compete with HS for precursor metabolites, such as nucleotide sugars and the sulfate donor 3′-phosphoadenosine-5′-phosphosulfate. Previous studies found that MST cells produced significant quantities of CS that was both stored intracellularly and secreted into the media (Gasimli et al., 2014). To quantitate the relative production of HS and CS, glycosaminoglycans derived from MST cell pellets were treated with heparin lyases or chondroitinase ABC and the remaining glycosaminoglycans were quantitated by carbazole assay. CS made up roughly 20% of the total purified glycosaminoglycan (Fig. 1c).

To streamline purification and eliminate the possibility of contamination, CS biosynthesis was genetically eliminated from the cell lines. The initial steps of HS and CS biosynthesis involve the assembly of a linkage tetrasaccharide attached to serine residues in core proteins after which CS biosynthesis diverges through the action of CS biosynthetic enzymes (Fig. 1a). RNA-Seq transcript analysis revealed that MST cells express CS biosynthetic enzymes CS N-acetylgalactosaminyltransferase 1 and 2 (Csgalnact1 and Csgalnact2), CS synthase 1 (Chsy1), and chondroitin polymerizing factor (Chpf) (Fig. 2a and biosynthetic pathway in Fig. 1a). In previous unpublished work, inactivation of Chpf using CRISPR/Cas9 gene targeting did not eliminate CS synthesis in CHO–S cells. Thus, CRISPR/Cas9 was used to simultaneously target *Csgalnact1*, *Csgalnact2* and *Chsy1* creating a mixed population called MST17 (see Fig. 4a). Screening 160 colonies by PCR identified five clones with all three genes mutated. Clone B10 had all three genes mutated as shown by PCR on genomic DNA (Fig. S2), lacked any CS (Fig. S3) and had the highest level of HS production (Fig. 2B). Interestingly, this CS knockout clone produced HS with moderately lower N-sulfate content and higher 6-O-sulfate content than wildtype MST (Fig. S4) although it is not clear if this change resulted from the CS knock out. Next generation sequencing of PCR amplicons generated from the mutated region of Csgalnact1 and Csgalnact2 revealed a predominant DNA sequence for each (95% and 90% of all amplicons, respectively) with an 81 amino acid deletion (residues 59–140) for Csgalnact1 and a 49 amino acid deletion (residues 102–151) for Csgalnact2. The mutations for each protein are located in the Golgi luminal portion of the protein. The remainder of each protein sequence was preserved. Sequencing of amplicons from wildtype cells was consistent with the mouse reference genome. Sequencing of the Chsy1 mutant amplicon was unsuccessful however all three genes appear to be mutated by the PCR analyses. Although we were unable to find evidence indicating whether these mutations eliminate glycosyltransferase activity, one or more of the enzymes must have been affected as CS production was eliminated (Fig. S3).

3.3. Engineering anticoagulant activity

Previous studies have reported the lack of 3-O-sulfate in MST HS and have shown that overexpression of Hs3st1 increased the anti-Xa activity

of fractionated MST HS from 20 U/mg to 50–60 U/mg (Montgomery et al., 1992; Gasimli et al., 2014); however, the US Pharmacopeia (USP) requirement for anti-Xa activity for pharmaceutical heparin is not less than 180 U/mg. Assuming that there may be other enzyme deficiencies, comparative gene expression profiling was employed to identify how MST cells differed from mast cells. Pharmaceutical heparin is derived from porcine intestinal mucosa, but porcine-derived mast cells were difficult to procure and data regarding porcine mast cell gene expression were unavailable. Transcript levels in murine mast cells could be compared directly with transcript levels in murine derived MST cells so bone marrow derived cells (BMDC) were collected from healthy mice and differentiated into mast cells. Mouse BMDC produced HS largely devoid of sulfate while HS from differentiated mast cells had higher sulfate content albeit only 64% of the sulfate content in pharmaceutical heparin (Fig. 3a and Fig. S5). Fractionation of crude porcine-derived heparin to enrich for anticoagulant activity likely accounts for the higher sulfate content in pharmaceutical heparin compared to the heparin purified from differentiated mast cells.

RNA-Seq analyses verified the lack of Hs3st1 expression in MST cells and showed that the expression level of Hs3st1 in differentiated mast cells was more than an order of magnitude higher than in BMDC (Fig. 3b). Transcriptomic analyses also confirmed that the other HS sulfotransferases were present at significant levels in the MST cells relative to heparin producing mast cells including Ndst1, Ndst2, Glce, Hs2st, Hs6st1 and Hs6st2 (Fig. 3b). Other enzymes involved in polymerization of the polysaccharide (Fig. S6a), metabolism and transport of activated sugar precursors (Fig. S6b) and HS core proteins (Fig. S6c) were also expressed. The placement of polymerases and sulfotransferases in the HS biosynthetic pathway is shown in Fig. 1a.

Since Hs3st1 overexpression was insufficient in previous engineering attempts to produce high anti-Xa activity in MST cells (Gasimli et al., 2014) and none of the other enzymes appeared to be lacking (Fig. 3b), we speculated that artificially high enzyme expression levels may be required in tissue culture to achieve heparin-like sulfate content and anticoagulant activity without fractionating the HS. Published analyses showing HS purified from Hs3st1-transduced MST cells suggest that overexpression of Hs3st1 produced sufficient 3-O-sulfation but may have lacked critical 6-O-sulfated residues (Gasimli et al., 2014). Our disaccharide composition analyses also indicated that 6-O-sulfate was lacking in MST cells compared to UFH (Fig. 1b). 2-O-sulfate is also reduced in MST cells compared to UFH, but it appears that 2-O-sulfate is not required for heparin's potent anticoagulant activity (Zhang et al., 2001). Our comparative expression analyses showed that Hs6st2 expression increases over 200-fold upon differentiation of BMDC to mast cells suggesting an important role for Hs6st2 in heparin production; however, MST cells already express levels of Hs6st1 and Hs6st2 similar to differentiated mast cells, so there may not be a bias for either of these enzymes in MST cells. Likewise, Ndst2 expression increased ten-fold
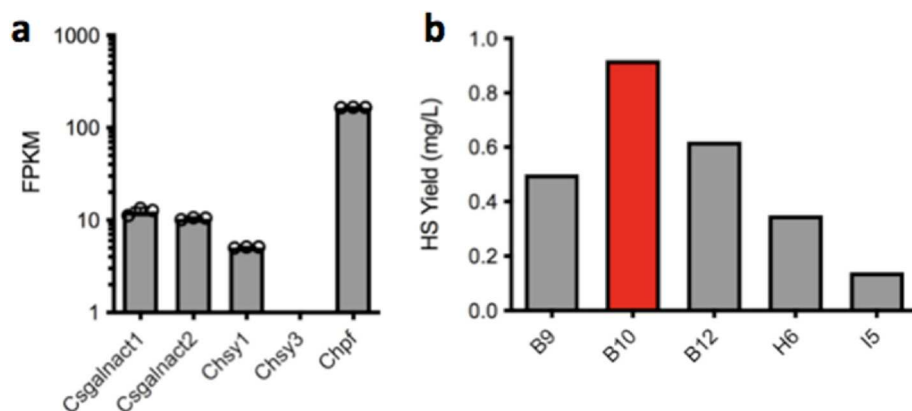

Fig. 2. Expression of CS biosynthetic enzymes and HS production by CS KO cell lines. a) RNA-Seq analysis of cultured WT MST cells was performed to determine the expression of genes responsible for production of CS (n = 3 independent samples). The expression of each transcript was calculated as FPKM. The position of these genes in the CS biosynthetic pathway is shown in Fig. 1a. b) Five MST17 colonies with Csgalnact1, Csgalnact2 and Chsy1 mutated were cultured under identical conditions. HS was purified and quantified from the cell pellet of each culture. Cell line shown in red was used for further engineering. Analysis was performed once for each cell line.
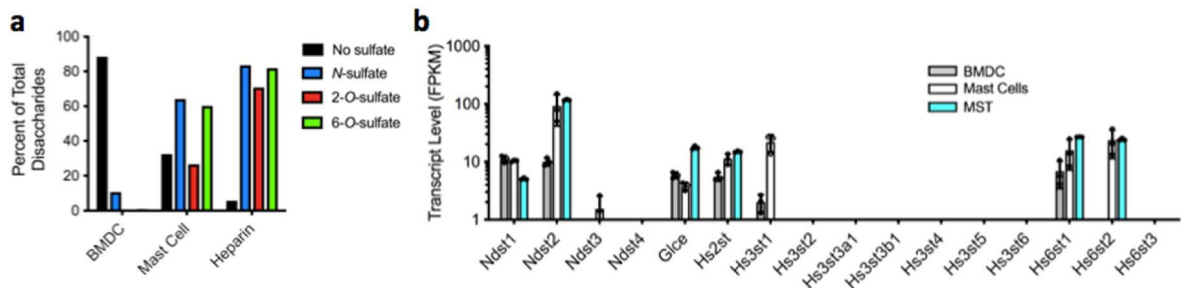
Fig. 3. Mast cells as a model for engineering recombinant heparin. a) BMDC were differentiated into mast cells over three weeks. HS was purified from precursor and differentiated cells and sulfate content was determined by LC/MS on the heparin lyase digested disaccharides. Analysis was performed once per cell type. Corresponding disaccharide composition data is shown in Fig. S5. b) RNA-Seq analysis was used to quantify HS biosynthetic enzyme transcripts from cultured BMDC, differentiated mast cells and MST cells. The position of each of these genes in the biosynthetic pathway is shown in Fig. 1a. (n = 3 independent samples each cell type).
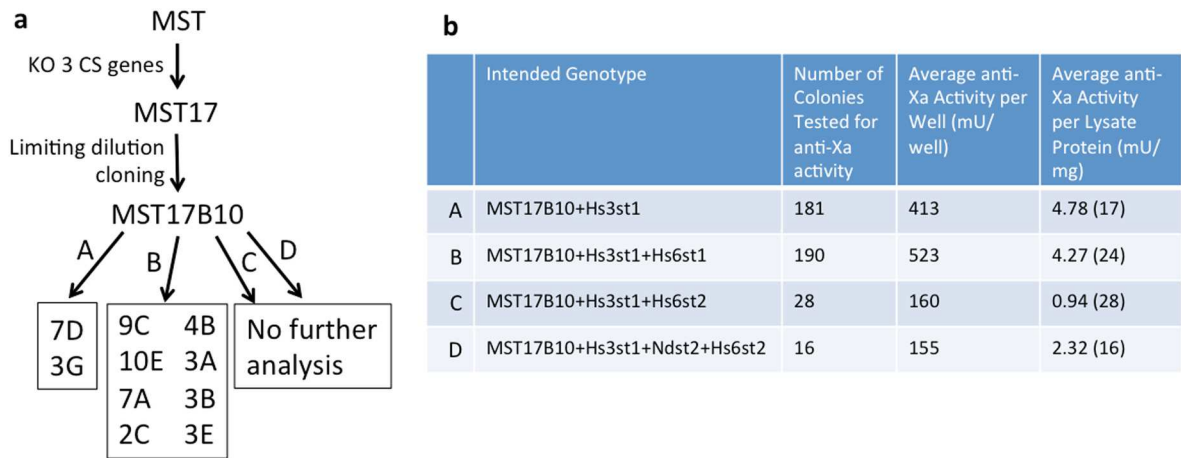
Fig. 4. Engineering MST cells. a) Lineage of engineered cell lines depicted. MST was targeted by CRISPR to knock out Csgalnact1, Csgalnact2 and Chsy1 creating the CS-deficient MST17 population. Limiting dilution cloning yielded MST17B10, which was subsequently transduced to overexpress combinations of sulfotransferases. The transductions depicted (A–D) are defined in the table. Cell lines from lineages C and D were not analyzed further due to low anti-Xa activity. The cell lines with the highest anti-Xa activity that were chosen for further characterization are shown in the boxes (e.g. A 7D, B 7A). b) Summary of single cell colonies analyzed from transductions of MST17B10. Colonies were initially genotyped by PCR to identify colonies with the intended genotype. The anti-Xa activity created by each colony in the 6-well dish and activity normalized by protein content of the lysate (for a subset number of the colonies) was determined from purified HS.

from BMDC to differentiated mast cells.

Based on these analyses, MST17B10 cells were transduced to overexpress Hs3st1 alone and in combination with Hs6st1, Hs6st2 and Ndst2 (Fig. 4a). Single cell colonies were isolated from the transduced populations by limiting dilution cloning and the genotypes were determined by PCR. HS was purified from these colonies grown in 6-well dishes in DME/F12 plus 15% FBS and was assayed for anti-Xa activity. Fig. 4b shows average anti-Xa activity per well for colonies from each combination of transduced genes. At first, total cellular protein was also measured for colonies to normalize for differences in cell number; however, the normalized values closely correlated with total activity in the wells, so total cellular protein was not measured in subsequent screening. In initial screening, the highest anti-Xa activities were observed in colonies transduced with Hs3st1 or Hs3st1 and Hs6st1 so additional colonies in those two groups were screened.

Colonies from each group were screened by PCR for the transgenes of interest (examples shown in Fig. S7). Expression of the transgenes at the transcript level was verified by RT-PCR on two representative colonies from each group (Fig. S8). Verification of protein expression was possible for Hs6st1 and Hs6st2 but the blots for Hs3st1 and Ndst2 were inconclusive (Fig. S9).

The ten colonies with the highest total anti-Xa activity/well were expanded into shaker flask cultures in DME/F12 medium plus 15% FBS for more extensive analysis. HS was purified and characterized from

both the cell pellet and conditioned medium in these cultures. HS yield (Fig. 5a) and anti-Xa specific activity (Fig. 5c) varied by cell line. Importantly, HS purified from the cell pellets exhibited high anti-Xa specific activity, in some cases exceeding 200 U/mg. Anti-Xa specific activity was considerably lower in HS purified from the cell culture medium; however, the yields of HS were typically higher from the medium than from the pellets (Fig. 5a).

3.4. Transition cells to serum-free medium

GMP production for use in humans requires that the cells be grown in serum-free medium. Colony B 3E was one of the first clones identified with high anticoagulant potency. To expedite selection of a defined medium in parallel with colony screening, these cells were transitioned to three commercial serum-free media and tested for cell growth (Fig. 6a), HS production (Fig. 6b), HS anti-Xa specific activity (Fig. 6c) and activity yield (Fig. 6d). CDM4NS0 was generally superior and so was chosen for further testing.

Growth of the candidate cell lines in CDM4NS0 resulted in a number of changes in HS production. In CDM4NS0, the yield of recombinant HS purified from the cell pellets increased compared to cells grown in DME/F12 + 15% FBS (Fig. 5a). The recombinant HS yields from the medium remained constant or decreased in excess of 50% among the different clones (Fig. 5a); however, the anti-Xa specific activity of HS purified
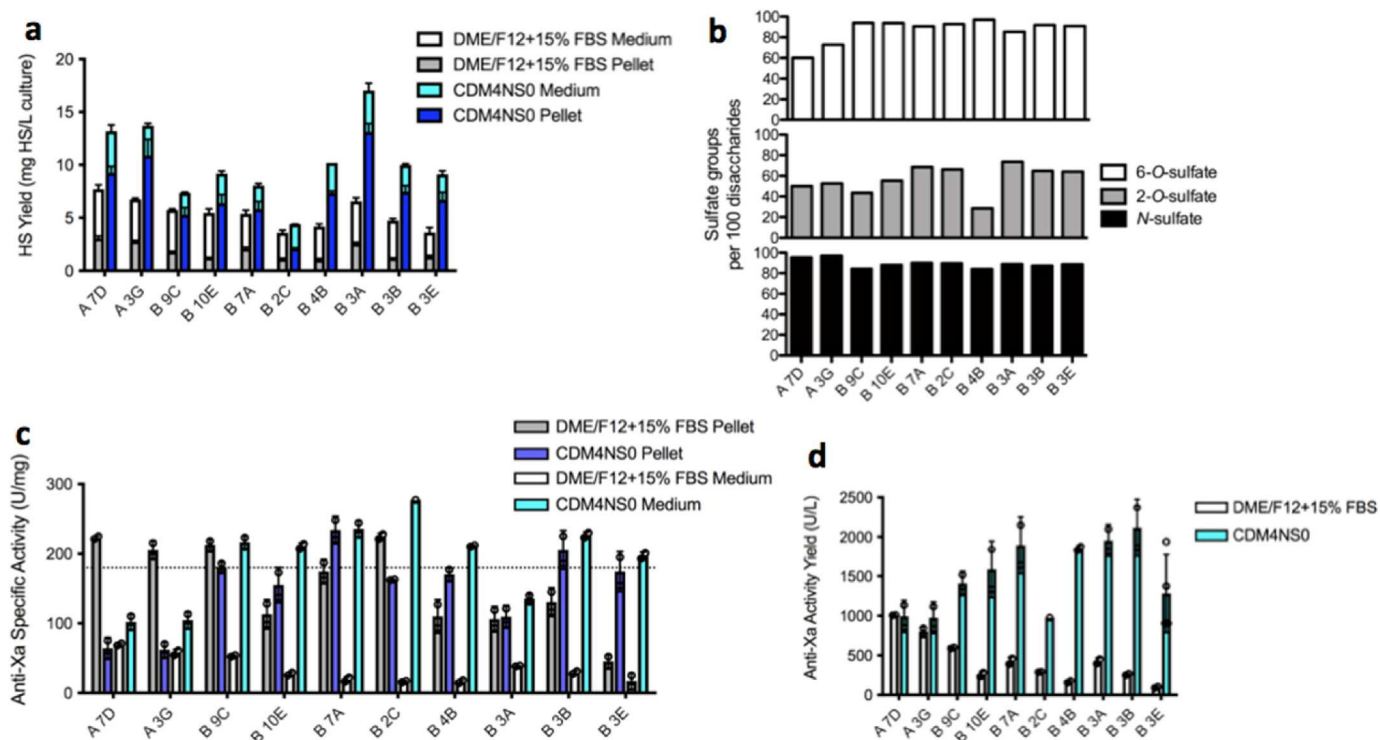
Fig. 5. Characterizing anticoagulant colonies. a) HS was purified from the cell pellet and the conditioned medium of candidate cell lines grown in DME/F12 plus 15% FBS or CDM4NS0 and quantified using the carbazole assay. Cell lines named "A" overexpress Hs3st1 while cell lines named "B" overexpress Hs3st1 and Hs6st1 as shown in Fig. 4b. b) Disaccharide analysis was performed to determine the sulfate content of HS produced in CDM4NS0. The corresponding disaccharide quantification is shown in Fig. S10. c) The anticoagulant potency was determined using the anti-Xa activity assay. d) The total anti-Xa activity yield from HS purified from both the cell pellet and the conditioned medium was determined using the carbazole assay and the anti-Xa activity assay. Samples were generated once and were assayed independently two or three times each.
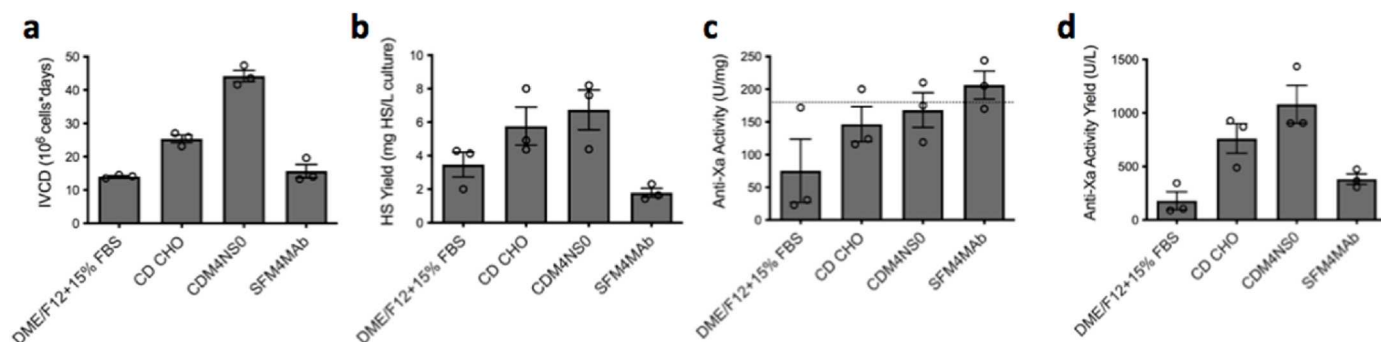

Fig. 6. Testing serum-free media. a) B 3E cells were grown in various media. Integrated viable cell density (IVCD) was determined over 7 days. b) HS was purified from these cells and total yield per volume of culture was determined by carbazole assay. c) The anti-Xa activity of purified HS was determined. The dotted line represents the USP anti-Xa requirement for UFH. d) The anti-Xa activity yielded per volume of culture medium was also determined. The experiment was performed twice with samples assayed twice per experiment.

from the medium increased in all clones and in some substantially (Fig. 5c). On the other hand, whereas anti-Xa specific activity in HS purified from the cell pellets remained constant or increased slightly in clones transduced with both Hs3st1 and Hs6st1 (B clones, Fig. 5c), the anti-Xa specific activity of HS purified from the cell pellets of cells transduced with only Hs3st1 decreased (A clones, Fig. 5c). Consistent with this finding, composition analyses showed lower levels of 6-O-sulfation in the cell lines transduced with only Hs3st1 compared to cell lines transduced with Hs3st1 and Hs6st1 (Fig. 5b and Fig. S10). Reduced anti-Xa activity may reflect a reduction of 6-O-sulfate groups, which are critical for activation of antithrombin, when the cells are grown in CDM4NS0.

Ultimately, the total recombinant heparin will be purified from both cell pellets and medium to produce the maximum yield of anti-Xa units.

Fig. 5d shows that the total yield of anti-Xa units was significantly increased in CDM4NS0 compared to DME/F12 plus 15% FBS for the clones transduced with Hs3st1 and Hs6st1 but was essentially unchanged for cell lines transduced with only Hs3st1. Importantly, 6 of 8 clones transduced with both Hs3st1 and Hs6st1 produced HS with anti-Xa specific activity equal to or above 180 U/mg (Fig. 5c).

Clone B 7A was chosen to more fully characterize the recombinant HS produced in serum-free medium because of the high anti-Xa specific activity in recombinant HS from both the cell pellet and the medium (Fig. 5c) and the relatively high overall yield of anti-Xa activity in CDM4NS0 (Fig. 5d). Clone B 7A achieved a maximum viable cell density of 9.6×10^6 cells/mL in 30 mL of CDM4NS0 plus 6 mM GlutaMAX (Figs. S11a and S11b). We also passaged the cell line out to 63 generations and discovered a 40% decrease of anti-Xa specific activity
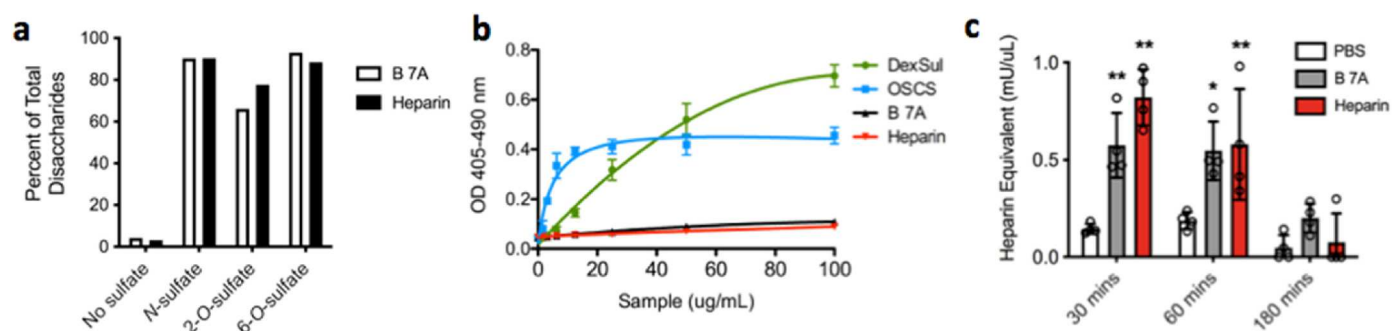
Fig. 7. Characterizing B 7A anticoagulant heparan sulfate. a) HS was purified from the cell pellet of B 7A cells grown in CDM4NS0. Sulfate content was determined once for each sample by UPLC analysis. The corresponding disaccharide composition is shown in Fig. S12. b) Test of activation of prekallikrein by B 7A HS with heparin, OSCS and dextran sulfate (DexSul) as controls. Experiment performed three times. c) Heparin (APP, 3 mg/kg), B 7A HS (3 mg/kg) or vehicle was administered via subcutaneous injection to mice (n = 4 each group). Blood was collected via tail bleed at 30, 60 and 180 min after injection. The anti-FXa activity in the plasma was measured and expressed in units of heparin activity. *p < 0.05, **p < 0.01 compared to PBS control.

compared to generation zero (Fig. S11c). Additional screening may reveal a more stable cell line. Reduction of anti-Xa activity may arise from reduction of transgene copy number or methylation of the CMV promoter that drives expression of the transgenes in our cell lines. In practice, about 24 generations will be needed to expand 10^7 frozen cells to 10^7 cells/mL in a 10,000 L bioreactor. At 24 generations, the anti-Xa activity of recombinant HS still exceeds the USP requirement for activity.

For continued characterization, clone B 7A was expanded in CDM4NS0 in multiple 1 L flasks and was allowed to grow for seven days before harvesting recombinant HS from the cell pellets and the medium separately. Recombinant HS yields from the cell pellet and the conditioned medium were 6.0 and 0.72 mg/L of culture volume, respectively. The recombinant HS purified from the cell pellets had sulfate content similar to UFH (Fig. 7a and Fig. S12) with 6-O-sulfate content notably higher than wildtype MST and 3-O-sulfate presence indicated by high anti-Xa activity. Recombinant heparin purified from the cell pellets was also assayed for potency and molecular weight by two different laboratories using heparin reference standards. As shown in Table 1, the anti-IIa and anti-Xa activity of Clone B 7A recombinant HS was >300 U/mg

and >280 U/mg, respectively, both higher than the USP requirement for UFH. Clone B 7A recombinant HS was larger (25.7 to 33.0 kDa) compared to the 16.7 kDa for the USP heparin standard (Table 1). B 7A recombinant HS also had potent heparin cofactor II activity (383 U/mg) as well as potent activity in the activated partial thromboplastin clotting time (APTT) assay (243 U/mg). When titrated against antithrombin, B 7A recombinant HS showed 64.8 percent high affinity material compared to 42.6 percent for UFH indicating that the cell engineering favored formation of antithrombin binding sites. OSCS activates prekallikrein and activation of the kinin system is likely responsible for deaths caused by contaminated heparin in 2008 (Kishimoto et al., 2008). Importantly, B 7A HS showed no activity in a kallikrein formation assay whereas OSCS and dextran sulfate (DexSul) elicited a strong response (Fig. 7b). B 7A HS performed similarly to UFH in vivo. Mice (n = 4) were administered a subcutaneous injection of B 7A HS, UFH or an equal volume of saline. Blood was collected into citrated tubes at 30, 60 and 180 min after injection and anti-Xa activity was determined in the plasma from each sample (Fig. 7c). Heparin and B 7A HS had similar effects and both significantly increased the anti-Xa activity in mouse plasma compared to PBS controls at 30 and 60 min.

4. Discussion

By combining gene expression profiling with multiplex genome engineering, we have engineered the biosynthetic pathway in MST cells to produce HS with potent anticoagulant activity. MST cells were used because the HS they produce is already highly sulfated, consistent with their derivation from mast cells (Montgomery et al., 1992). Although highly sulfated, MST cells lack Hs3st1 expression, a critical enzyme for creation of the antithrombin binding site. Hs3st1 has been overexpressed previously in MST cells; however, the anti-Xa activity reported in those studies was still significantly below the USP criteria for pharmaceutical heparin (Gasimli et al., 2014). This suggests that other tissue factors not found in the cell culture environment may normally stimulate mast cells to produce sufficient anticoagulant activity for pharmaceutical heparin. In the cell culture environment, artificially high enzyme expression levels appear to be required.

In previous work, HS from MST cells transduced with Hs3st1 was analyzed for the presence of antithrombin binding sites by tetrasaccharide analyses following heparin lyase II digestion (Gasimli et al., 2014). Five heparin lyase resistant tetrasaccharides containing 3-O-sulfate were identified matching the five tetrasaccharides found in bovine heparin. While the abundance of 3-O-sulfate in tetrasaccharides from transduced cells appeared sufficient, over half of the tetrasaccharides from transduced cells lacked a 6-O-sulfate group that is critical for binding antithrombin and for anti-Xa activity. 6-O-sulfate on the non-reducing end GlcNAc of the antithrombin binding

Table 1
Characterization of B 7A HS including APTT, factor Xa and factor IIa inhibition, heparin cofactor II (HCII) activity, molecular weight and percent of material containing a high affinity binding site for antithrombin in comparison to the UFH standards.

	International Standard[a,b]		USP Standard[a]		USP Criteria
	B 7A HS	UFH	B 7A HS	UFH	
APTT (U/mg)	243 (239–247)	199 (189–209)			NA
Anti-Xa (U/mg)	281 (259–304)	203 (187–219)	297	197	≥180
Anti-IIa (U/mg)	366 (359–374)	196 (176–218)	311	209	≥180
Anti-Xa/Anti-IIa	0.77 (0.69–0.85)	1.04 (0.86–1.24)	0.95	0.94	0.9–1.1
HCII (U/mg)	383 (371–396)	206 (197–216)			NA
Weight average MW (kDa)	33.0	16.7	25.7	16.5	15–19
Polydispersity	1.59	1.23	1.33	1.25	NA
% High affinity material	64.8 (SD ± 3.4)	42.6 (SD ± 2.6)			NA

[a] Analysis with the International heparin standard or the USP reference standard were performed at two independent laboratories.

[b] Values shown with the International Standard are averages with 95% confidence intervals shown in parenthesis where appropriate for three separate experiments on a single preparation of material.

pentasaccharide is the second most important sulfate group as this, together with the 3-*O*-sulfate, is responsible for over half of the anti-thrombin binding energy (Atha et al., 1985). Thus, despite significant levels of Hs6st1 and Hs6st2 transcripts in MST cells, overexpression of Hs3st1 was here combined with overexpression of Hs6st1 and/or Hs6st2.

The high anti-Xa activity in the colonies transduced exclusively with Hs3st1 confirms the importance of 3-*O*-sulfation (Atha et al., 1985) and suggests that transduced Hs3st1 gene dosage may be a determining factor. Higher anti-Xa specific activities observed here relative to prior work may reflect differences in growth conditions (stationary cultures vs. shaker flasks) or genetic differences (clonal variations or transduction efficiencies by lentivirus vs. retrovirus). Interestingly, Hs6st1 transduction appeared to enhance anti-Xa activity more than Hs6st2. Both enzymes can modify GlcNS residues flanked by 2-*O*-sulfated IdoA residues (Kreuger and Kjellen, 2012; Smeds et al., 2003; Jemth et al., 2003); however, HS6ST1 preferentially catalyzes the sulfation of the IdoA-GlcNS disaccharide unit, whereas HS6ST2 prefers the GlcA-GlcNS and IdoA(2S)-GlcNS disaccharides (Habuchi et al., 2000, 2003; Nagai et al., 2007). Gene knockout studies have indicated that Ndst2 is essential for heparin biosynthesis (Kreuger and Kjellen, 2012; Forsberg et al., 1999; Humphries et al., 1999); however, Ndst2 transduction did not result in increased anti-Xa activity indicating that the HS is adequately *N*-sulfated by the endogenous enzymes.

Differences in activity were observed between HS purified from cell pellets and from conditioned medium. Like mast cells, MST cells have little or no glycosaminoglycans on their surfaces but have intracellular granules that store glycosaminoglycans (Montgomery et al., 1992). Mast cells degranulate and release the granule contents when multivalent antigens crosslink antigen specific IgE bound to high affinity IgE receptors on mast cell surfaces. Mast cells also release granule contents by constitutive exocytosis. Similarly, MST cells grown in suspension without agitation released about 10% of their HS into the cell culture medium (Montgomery et al., 1992; Gasimli et al., 2014). Higher levels of recombinant heparin in the medium in our studies may have been due to swirling in the shaker flasks.

Commercial production will require that the cells be grown in serum-free medium for administering the recombinant heparin to humans. Our studies showed that CDM4NS0, a commercial serum-free medium, increased the production of total polysaccharide material/liter of cell culture medium, anti-Xa activity/liter of cell culture medium and anti-Xa specific activity. When cells were transitioned to CDM4NS0, HS from clones transduced with Hs3st1 and Hs6st1 maintained high anti-Xa specific activity and 6-*O*-sulfate content while activity and 6-*O*-sulfate content in HS from clones transduced with Hs3st1 only decreased substantially (Fig. 5b and c). Reduced anti-Xa activity may have been caused by reduced 6-*O*-sulfate, which is critical for the high affinity of the antithrombin binding pentasaccharide (Atha et al., 1985). Although little is known about transcriptional regulation of the HS biosynthetic enzymes, these findings suggest that there may be a serum factor that influences the extent of 6-*O*-sulfation. Overexpression of Hs6st1 with a constitutive promoter driving expression of the transduced gene likely uncoupled 6-*O*-sulfation from influences in the medium.

Two independent laboratories characterized the HS produced by the B 7A cell line. Differences in their measurements likely arose from different test methods and standards. Nevertheless, their results were largely consistent with B 7A HS having greater anticoagulant potency and longer chain length than USP specifications. Notably, like heparin, B 7A HS inhibits factor IIa and factor Xa through antithrombin, and factor IIa through heparin cofactor II, without activating the kinin system through kallikrein. Heparin accelerates antithrombin's inactivation of thrombin by serving as a template that approximates and orients the proteins so the longer chain length of B 7A HS compared to heparin may be responsible for the greater anti-IIa activity over anti-Xa activity (Table 1). Reducing the chain length may help balance the ratio to match USP specifications, increase the half-life in circulation and reduce

the risk of heparin-induced thrombocytopenia as observed for low molecular weight heparin. Transcript analysis revealed that MST cells do not express heparanase, a secreted enzyme that cleaves HS at specific sites within the chain. Overexpression of the enzyme may produce shorter HS chains.

To our knowledge this is the first demonstration of recombinant HS production from an engineered mammalian cell line with anticoagulant potency equaling or exceeding pharmaceutical heparin. This illustrates the feasibility of a synthetic biology approach to substitute for animal derived heparin. Further bioprocess research is aimed at increasing scale and production efficiency. Additional genetic engineering is also directed toward heparin with superior properties such as reduced risk of side effects.

Data availability

The RNA-Seq datasets generated during the current study are available at the NCBI Sequence Read Archive with the BioProject accession number PRJNA763926.

Author statement

Bryan Thacker: Conceptualization, Methodology, Investigation, Writing – Original Draft, Writing – Review and Editing, Visualization, Supervision, Project Administration, Funding Acquisition. Kristen Thorne, Colin Cartwright, Jeeyoung Park, Kimberly Glass, Annie Chea, Zhenping Wang: Investigation, Validation. Benjamin Kellman: Formal analysis. Walter Jeske, John Hogwood: Investigation, Formal Analysis, Writing – Review and Editing. Nathan Lewis, Anna Di Nardo, Susan Sharfstein, Jeanine Walenga, Elaine Gray, Barbara Mulloy and Jeffrey Esko: Conceptualization, Writing – Review and Editing. Charles Glass: Conceptualization, Writing – Original Draft, Writing – Review and Editing, Supervision, Project Administration, Funding Acquisition.

Declarations of competing interest

J.D.E. and C.A.G. are cofounders of TEGA Therapeutics, Inc. and hold equity positions in the company. C.A.G., B.E.T., C.C., J.P. are employees of TEGA Therapeutics, Inc. and own stock or stock options. B.P.K. and N. E.L. hold stock in the company. S.T.S. is the recipient of a subcontract from TEGA Therapeutics related to bioproduction of recombinant heparin.

Appendix A. Supplementary data

Supplementary data to this article can be found online at https://doi.org/10.1016/j.ymben.2022.01.002.

References

Ahsan, A., Jeske, W., Hoppensteadt, D., Lormeau, J.C., Wolf, H., Fareed, J., 1995. Molecular profiling and weight determination of heparins and depolymerized heparins. J. Pharm. Sci. 84, 724–727.

Atha, D.H., Lormeau, J.C., Petitou, M., Rosenberg, R.D., Choay, J., 1985. Contribution of monosaccharide residues in heparin binding to antithrombin III. Biochemistry 24, 6723–6729.

Baik, J.Y., Gasimli, L., Yang, B., Datta, P., Zhang, F., Glass, C.A., Esko, J.D., Linhardt, R. J., Sharfstein, S.T., 2012. Metabolic engineering of Chinese hamster ovary cells: towards a bioengineered heparin. Metab. Eng. 14, 81–90.

Bitter, T., Muir, H.M., 1962. A modified uronic acid carbazole reaction. Anal. Biochem. 4, 330–334.

Bolger, A.M., Lohse, M., Usadel, B., 2014. Trimmomatic: a flexible trimmer for Illumina sequence data. Bioinformatics 30, 2114–2120.

Church, D.M., Schneider, V.A., Graves, T., Auger, K., Cunningham, F., Bouk, N., Chen, H. C., Agarwala, R., McLaren, W.M., Ritchie, G.R., Albracht, D., Kremitzki, M., Rock, S., Kotkiewcz, H., Kremitzki, C., Wollam, A., Trani, L., Fulton, L., Fulton, R., Matthews, L., Whitehead, S., Chow, W., Torrance, J., Dunn, M., Harden, G., Threadgold, G., Wood, J., Collins, J., Heath, P., Griffiths, G., Pelan, S., Grafham, D., Eichler, E.E., Weinstock, G., Mardis, E.R., Wilson, R.K., Howe, K., Flicek, P., Hubbard, T., 2011. Modernizing reference genome assemblies. PLoS Biol. 9, e1001091.

Committee on Energy and Commerce, C.O.T. US (2016 – 2018) Letters ot the Honeoarble Robvert M Califf MD abd The Honorable Scott Gottlieb, MD; Commisioners of the Food and Drug Administration, Washington DC. https://energycommerce.house. gov/news/letter/letter-fda-regarding-fraud-concerns-china-possible-u-s-heparin-sh ortage/.

Deakin, J.A., Lyon, M., 2008. A simplified and sensitive fluorescent method for disaccharide analysis of both heparan sulfate and chondroitin/dermatan sulfates from biological samples. Glycobiology 18, 483–491.

Dobin, A., Davis, C.A., Schlesinger, F., Drenkow, J., Zaleski, C., Jha, S., Batut, P., Chaisson, M., Gingeras, T.R., 2013. STAR: ultrafast universal RNA-seq aligner. Bioinformatics 29, 15–21.

Forsberg, E., Pejler, G., Ringvall, M., Lunderius, C., Tomasini-Johansson, B., Kusche-Gullberg, M., Eriksson, I., Ledin, J., Hellman, L., Kjellen, L., 1999. Abnormal mast cells in mice deficient in a heparin-synthesizing enzyme. Nature 400, 773–776.

Gasimli, L., Glass, C.A., Datta, P., Yang, B., Li, G., Gemmill, T.R., Baik, J.Y., Sharfstein, S. T., Esko, J.D., Linhardt, R.J., 2014. Bioengineering murine mastocytoma cells to produce anticoagulant heparin. Glycobiology 24, 272–280.

Glass, C.A., 2018. Recombinant heparin-new opportunities. Front. Med. 5, 341.

Habuchi, H., Tanaka, M., Habuchi, O., Yoshida, K., Suzuki, H., Ban, K., Kimata, K., 2000. The occurrence of three isoforms of heparan sulfate 6-O-sulfotransferase having different specificities for hexuronic acid adjacent to the targeted N-sulfoglucosamine. J. Biol. Chem. 275, 2859–2868.

Habuchi, H., Miyake, G., Nogami, K., Kuroiwa, A., Matsuda, Y., Kusche-Gullberg, M., Habuchi, O., Tanaka, M., Kimata, K., 2003. Biosynthesis of heparan sulphate with diverse structures and functions: two alternatively spliced forms of human heparan sulphate 6-O-sulphotransferase-2 having different expression patterns and properties. Biochem. J. 371, 131–142.

Hogwood, J., Naggi, A., Torri, G., Page, C., Rigsby, P., Mulloy, B., Gray, E., 2018. The effect of increasing the sulfation level of chondroitin sulfate on anticoagulant specific activity and activation of the kinin system. PLoS One 13, e0193482.

Huang, Y., Mao, Y., Zong, C., Lin, C., Boons, G.J., Zaia, J., 2015. Discovery of a heparan sulfate 3-O-sulfation specific peeling reaction. Anal. Chem. 87, 592–600.

Humphries, D.E., Wong, G.W., Friend, D.S., Gurish, M.F., Qiu, W.T., Huang, C., Sharpe, A.H., Stevens, R.L., 1999. Heparin is essential for the storage of specific granule proteases in mast cells. Nature 400, 769–772.

Jemth, P., Smeds, E., Do, A.T., Habuchi, H., Kimata, K., Lindahl, U., Kusche-Gullberg, M., 2003. Oligosaccharide library-based assessment of heparan sulfate 6-O-sulfotrans-ferase substrate specificity. J. Biol. Chem. 278, 24371–24376.

Keire, D., Mulloy, B., Chase, C., Al-Hakim, A., Cairatti, D., Gray, E., et al., 2015. Diversifying the global heparin supply chain: reintroduction of bovine heparin in the United States. Pharmaceut. Technol. 39, 28–35.

Kishimoto, T.K., Viswanathan, K., Ganguly, T., Elankumaran, S., Smith, S., Pelzer, K., Lansing, J.C., Sriranganathan, N., Zhao, G., Galcheva-Gargova, Z., Al-Hakim, A., Bailey, G.S., Fraser, B., Roy, S., Rogers-Cotrone, T., Buhse, L., Whary, M., Fox, J., Nasr, M., Dal Pan, G.J., Shriver, Z., Langer, R.S., Venkataraman, G., Austen, K.F., Woodcock, J., Sasisekharan, R., 2008. Contaminated heparin associated with adverse clinical events and activation of the contact system. N. Engl. J. Med. 358, 2457–2467.

Kreuger, J., Kjellen, L., 2012. Heparan sulfate biosynthesis: regulation and variability. J. Histochem. Cytochem. 60, 898–907.

Lawrence, R., Olson, S.K., Steele, R.E., Wang, L., Warrior, R., Cummings, R.D., Esko, J.D., 2008a. Evolutionary differences in glycosaminoglycan fine structure detected by quantitative glycan reductive isotope labeling. J. Biol. Chem. 283, 33674–33684.

Lawrence, R., Lu, H., Rosenberg, R.D., Esko, J.D., Zhang, L., 2008b. Disaccharide structure code for the easy representation of constituent oligosaccharides from glycosaminoglycans. Nat. Methods 5, 291–292.

Lord, M.S., Cheng, B., Tang, F., Lyons, J.G., Rnjak-Kovacina, J., Whitelock, J.M., 2016. Bioengineered human heparin with anticoagulant activity. Metab. Eng. 38, 105–114.

Mans, D.J., Ye, H., Dunn, J.D., Kolinski, R.E., Long, D.S., Phatak, N.L., Ghasriani, H., Buhse, L.F., Kauffman, J.F., Keire, D.A., 2015. Synthesis and detection of N-sulfonated oversulfated chondroitin sulfate in marketplace heparin. Anal. Biochem. 490, 52–54.

Market Report, 2020. The Risk of African Swine Fever in the US and Australia – June 2020. The Pig Site July 8. Global Ag Media. https://www.thepigsite.com/contr ibutors/global-ag-media-2.

McMahon, A.W., Pratt, R.G., Hammad, T.A., Kozlowski, S., Zhou, E., Lu, S., Kulick, C.G., Mallick, T., Dal Pan, G., 2010. Description of hypersensitivity adverse events following administration of heparin that was potentially contaminated with oversulfated chondroitin sulfate in early 2008. Pharmacoepidemiol. Drug Saf. 19, 921–933.

Montgomery, R.I., Lidholt, K., Flay, N.W., Liang, J., Vertel, B., Lindahl, U., Esko, J.D., 1992. Stable heparin-producing cell lines derived from the Furth murine mastocytoma. Proc. Natl. Acad. Sci. U. S. A. 89, 11327–11331.

Mulloy, B., Heath, A., Shriver, Z., Jameison, F., Al Hakim, A., Morris, T.S., Szajek, A.Y., 2014. USP compendial methods for analysis of heparin: chromatographic determination of molecular weight distributions for heparin sodium. Anal. Bioanal. Chem. 406, 4815–4823.

Nagai, N., Habuchi, H., Kitazume, S., Toyoda, H., Hashimoto, Y., Kimata, K., 2007. Regulation of heparan sulfate 6-O-sulfation by beta-secretase activity. J. Biol. Chem. 282, 14942–14951.

Oduah, E.I., Linhardt, R.J., Sharfstein, S.T., 2016. Heparin: past, present, and future. Pharmaceuticals 9.

Smeds, E., Habuchi, H., Do, A.T., Hjertson, E., Grundberg, H., Kimata, K., Lindahl, U., Kusche-Gullberg, M., 2003. Substrate specificities of mouse heparan sulphate glucosaminyl 6-O-sulphotransferases. Biochem. J. 372, 371–380.

Thacker, B.E., Sharfstein, S.T., 2018. Metabolic engineering of mammalian cells to produce heparan sulfates. Emerg. Top Life Sci. 2, 443–452.

Thacker, B.E., Xu, D., Lawrence, R., Esko, J.D., 2014. Heparan sulfate 3-O-sulfation: a rare modification in search of a function. Matrix Biol. 35, 60–72.

Wang, Z., Lai, Y., Bernard, J.J., Macleod, D.T., Cogen, A.L., Moss, B., Di Nardo, A., 2012. Skin mast cells protect mice against vaccinia virus by triggering mast cell receptor S1PR2 and releasing antimicrobial peptides. J. Immunol. 188, 345–357.

WHO Model List of Essential Medicines - 21st List, 2019. WHO Reference Number: WHO/MVP/EMP/IAU/2019.06. Copyright CC BY-NC-SA 3.0 IGO.

Xu, D., Esko, J.D., 2014. Demystifying heparan sulfate-protein interactions. Annu. Rev. Biochem. 83, 129–157.

Zhang, L., Lawrence, R., Schwartz, J.J., Bai, X., Wei, G., Esko, J.D., Rosenberg, R.D., 2001. The effect of precursor structures on the action of glucosaminyl 3-O-sulfo-transferase-1 and the biosynthesis of anticoagulant heparan sulfate. J. Biol. Chem. 276, 28806–28813.